Biomimetic self-assembly of helical electrical circuits using orthogonal capillary interactions

David H. Gracias, Mila Boncheva, Osahon Omoregie, and George M. Whitesides[a)]
Department of Chemistry and Chemical Biology, Harvard University, Cambridge, Massachusetts 02138

(Received 20 December 2001; accepted for publication 17 February 2002)

This letter describes the biomimetic self-assembly of mm-sized polyhedra into helical aggregates. The system used two orthogonal, capillary interactions that acted in parallel. The design of the self-assembly process, and of the resulting structures, was modeled on the formation and structure of tobacco mosaic virus. The self-assembled, helical aggregates carried one, two, or four isolated, electrical circuits. © *2002 American Institute of Physics.* [DOI: 10.1063/1.1470222]

Self-assembly occurs throughout biological systems, and in most cases results in the formation of three-dimensional (3D) structures.[1] Viewed from the vantage of a designer, these biological processes incorporate three major design concepts: (1) shape recognition, to position the components correctly in an aggregate; (2) simultaneous or sequential operation of interactions in 3D, to strengthen the aggregate; and (3) entropic constraint, to minimize the formation of defects in the self-assembled structures. This letter illustrates the use of concepts abstracted from biological self-assembly in the fabrication of mesoscale 3D aggregates that form helical electrical circuits. The examples we describe were modeled on the structure and self-assembly of tobacco mosaic virus (TMV).[2,3]

TMV comprises a strand of ribonucleic acid (RNA), surrounded by a protein coat. The protein subunits are arranged in a single, right-handed helix; the RNA strand intercalates between the adjacent turns of the protein helix. The self-assembly of the virus results from finely balanced, orthogonal weak interactions between the protein molecules and the RNA; these interactions operate both along the lateral and the longitudinal directions of the viral helix. The assembly proceeds in two stages: nucleation and elongation. During the initial, nucleation stage, the protein molecules assemble by hydrogen bonds, electrostatic, and hydrophobic interactions into small, two-layer disks (nuclei). During the elongation stage, these protein disks bind electrostatically, one at the time, to a hairpin loop in the RNA strand, and anneal into a single, helical aggregate.

The basic units of the self-assembling system we describe were wedge-shaped polyhedra made of organic polymer (polyurethane), with dimensions of several millimeters; these polyhedra serve as analogues of the protein molecules in TMV. The orthogonal faces of the polyhedra carried patterns of solder (Bi–Pb–In–Sn–Cd alloy, mp 47 °C), and hydrophobic lubricant (perfluorodecalin, PFD); these patterns provide the information necessary for the self-assembly of the system, and serve as analogues of the functional groups along the side chains of the protein of TMV involved in the virus assembly. Upon self-assembly, the polyhedra organized into a helix via two capillary forces: a strong capillary interaction between drops of molten solder[4] (the free energy of the water–solder interface is ~ 400 ergs/cm^2), and a relatively weak capillary interaction between drops of PFD[5] (the free energy of the PFD–water interface is ~ 50 ergs/cm^2). The system was designed in such a way that these two forces were orthogonal to each other, mimicking the forces generating the TMV helix. The polyhedra interacted laterally through drops of molten solder; this interaction mimics the lateral interaction between adjacent protein molecules in the TMV helix. Along the main helix axis, the polyhedra interacted through drops of hydrophobic lubricant; this interaction mimics the electrostatic interaction between the protein disks and RNA in the virus.

We fabricated the polyhedra by molding a photocurable polymer (polyurethane) in poly(dimethylsiloxane) molds.[4,6] Masters for molding were prepared by conventional machining in aluminum. Patterns of copper that provided the basis for the electrical circuits were defined using photolithography on a copper–polyimide laminate (Pyralux-LF9110, DuPont), as previously described.[7] Pieces of polymer film supporting the copper patterns were cut out and glued onto the faces of the polyhedra.

Figure 1(a) shows schematically a wedge-shaped polyhedron, the basic unit of the self-assembling system. The geometry of the wedge was chosen to result in formation of helices with defined handedness upon assembly. When the wedges interacted by their chiral sides [indicated with arrows in Fig. 1(b)], each piece occupied a sector of 66° when projected along the helix axis; thus, assembly of six pieces resulted in 1.1 turns of a helix [Fig. 1(c)].

The faces of each wedge were patterned as shown in Figs. 1(e) and 2(b): (a) three faces carried a copper pattern of contact pads and wires; (b) two faces of the wedge were hydrophobic; and (c) one face of the wedge was covered by polyimide and did not participate in the self-assembly process.

The component wedges were patterned, dipped in molten solder and dipped in PFD. The solder covered the copper pattern selectively, while PFD covered the hydrophobic faces of the wedges. The pieces were then placed in aqueous KBr solution that was approximately isodense. The *p*H of the solution was adjusted to ~ 3 with acetic acid, to dissolve the oxides formed on the surface of the solder on contact with air and water. The suspension was heated to 60 °C, and tumbled

a)Author to whom all correspondence should be addressed; electronic mail: gwhitesides@gmwgroup.harvard.edu

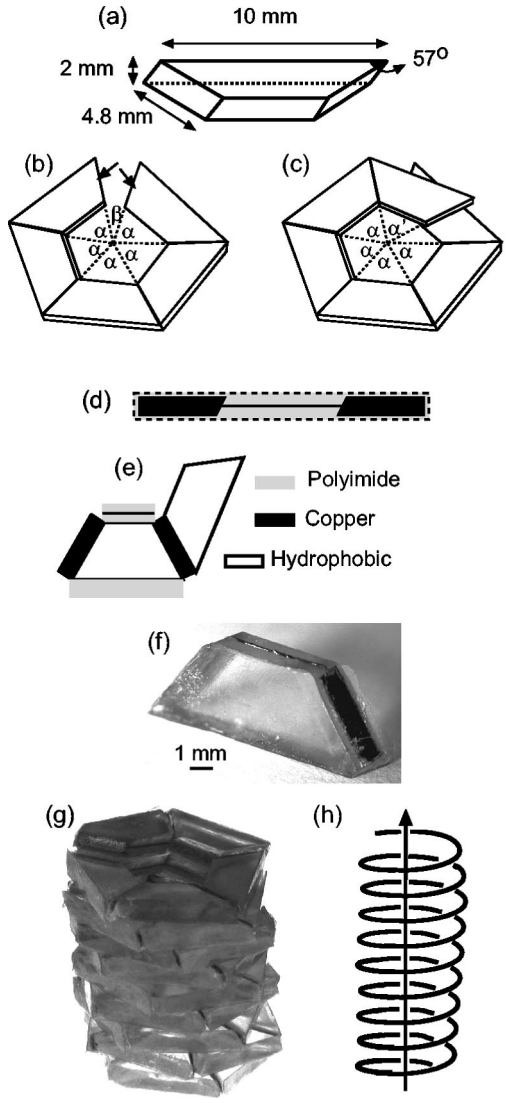

FIG. 1. Design of the basic unit of the helical assemblies. (a) Schematic drawing of a wedge-shaped polyhedron. (b) A drawing of an aggregate containing five wedges. The coplanar angles α and β have values of 66° and 30°, respectively. The arrows indicate the two possible binding sites for an incoming wedge. (c) A drawing of an aggregate containing six wedges. The angle α' is out of plane with respect to the angles α, and has a value of 66°. Helical assembly carrying one electrical circuit: (d) The pattern of copper used (single-wire pattern). (e) The patterned wedge. (f) A single wedge after solder deposition, prior to assembly. (g) A photograph of a helix formed from 48 pieces. (h) Schematic diagram of the helical electrical circuit.

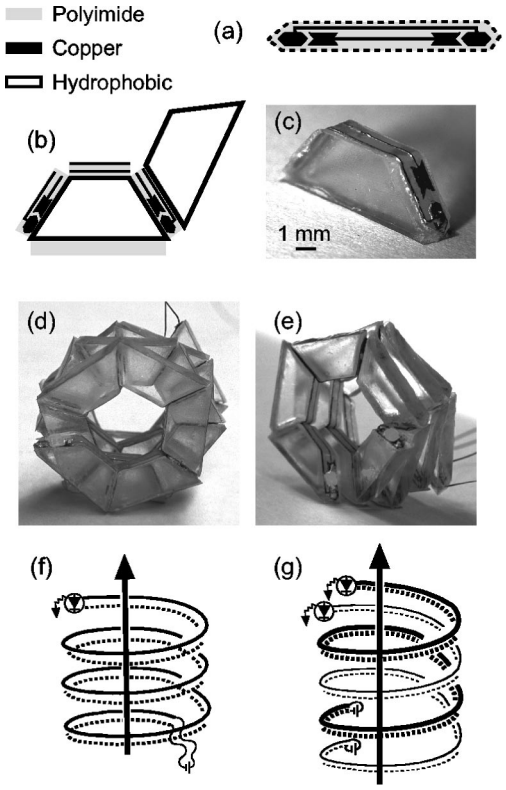

FIG. 2. Helical assemblies carrying several electrical circuits. (a) The pattern of copper used (dual-wire pattern). (b) The patterned wedge. (c) A single wedge after solder deposition, prior to self-assembly. (d) A photograph of a helix formed from 20 pieces, carrying one pair of electrically isolated wires. (e) A photograph of two interdigitated helices, one formed from seven pieces, the other one from ten pieces. Each helix carries a pair of electrically isolated wires. (f), (g) Schematic diagram of the electrical circuits formed in (d) and (e), respectively.

using a rotary evaporator. Self-assembly occurred when pieces collided with each other and either drops of solder, or drops of PFD, coalesced. The two types of capillary interactions seemed not to interfere. Different runs of the self-assembly experiments resulted in topologically identical structures, although the number of pieces in the formed aggregates varied by 2%–5%.

In generating helices, we used two kinds of patterns. One pattern consisted of two rectangular contact pads connected by a wire [a single-wire pattern, Fig. 1(d)]. The self-assembly was carried out for 1 h with a total of 75 patterned pieces [Figs. 1(e) and 1(f)]. The small, helical loops that formed initially (containing $\sim 6-8$ wedges) interacted via drops of PFD and formed a single-helical aggregate [containing 48 pieces; Fig. 1(g)]. The aggregate carried a single wire running across the pieces [Fig. 1(h)]. The lateral stacking between adjacent turns of the helix strengthened the structure against the disruptive shear during agitation and assembly. In the absence of PFD, we were not able to grow aggregates larger than 14 pieces (also starting with 75 pieces, and allowing the assembly to proceed for 1 h).

The second pattern of contact pads and wires we used is shown in Fig. 2(a). It contained a pair of electrically isolated wires (a dual-wire pattern). Each wire was connected to two contact pads. Self-assembly of wedges carrying this pattern [Figs. 2(b) and 2(c)] generated two different kinds of aggregates with approximately equal yield. One consisted of a single helix, carrying a pair of electrically isolated wires [Figs. 2(d) and 2(f)]; the other consisted of two interdigitated helices carrying two pairs of electrically isolated wires [Figs. 2(e) and 2(g)]. We verified the continuity of the electrical interconnections in these aggregates by connecting one end of the helix to a battery and the second end to a light-emitting diode (LED) (American Bright Optoelectronics Corp.). The formation of interdigitated helices suggests that in this system the overall strength of the capillary interactions involving PFD exceeded the overall strength of those involving solder.

In previous examples of mesoscale self-assembly, the systems were based on only one type of interaction: capillary forces between films of hydrophobic liquid[8–10] or drops of molten solder,[11,12] magnetic forces,[13] electrostatic forces,[14] or optical fields.[15] We have described the mesoscale self-

assembly of mm-sized objects in two-dimensions (2D) in a system using a combination of hydrodynamic and magnetic forces.[16] In the present work, we show that it is possible to combine several capillary interactions in a 3D system. We believe that it is furthermore possible to design a 3D system that uses a combination of forces of a different origin, e.g., capillary, electrostatic, and magnetic.

Systems of orthogonal interactions are especially relevant for fabricating 3D, self-assembled aggregates that can act as components in functional devices (e.g., microelectronic, photonic, microelectromechanical systems). In order to perform a specific function, such assemblies must comprise complex (often asymmetrical) networks of connections providing structural connectivity between the elements, together with connections carrying the functional (e.g., electrical or optical) signals, both between the components, and between groups of different components. The use of orthogonal forces in 3D allows one to build more robust structures and structures of higher complexity. Moreover, a system employing orthogonal interactions makes it possible to build multifunctional assemblies, i.e., structures in which the orthogonal connections between the elements can carry electrical or optical function. The assembly process can be designed to use the orthogonal interactions simultaneously (as in the present example) or consecutively.

The biological system we modeled in this work, TMV, is far more sophisticated than the one we describe: it consists of two different types of molecules (protein and RNA), while we used identical, mm-sized components; the molecular components change their orientation upon assembly (the protein disks transform into a helix upon binding to RNA); multitude of forces of different origin act during the virus assembly process (e.g., hydrogen bonds, electrostatic, and hydrophobic interactions), while in our system, we used only capillary interactions. The system we have described does, however, illustrate the abstraction of ideas from TMV assembly, and the application of these ideas to the design of self-assembling aggregates of complex geometry. Biological systems offer a wealth of structural features and self-assembling structures that can be explored. We believe that as alternative methods for the fabrication of 3D functionalized components are being developed,[17] the abstraction of biological principles will prove to be of great value for the development of artificial self-assembling systems.

This work was supported by grants from NSF and DARPA.

[1] L. Stryer, *Biochemistry* (Freeman, New York, 1995).
[2] A. Klug, Angew. Chem. **95**, 579 (1983).
[3] A. C. Bloomer and P. J. G. Butler, in *The Plant Viruses*, edited by M. H. V. Van Regenmortel and H. Fraenkel-Conrat (Plenum, New York, 1986), Vol. 2, p. 19.
[4] T. L. Breen, J. Tien, S. R. J. Oliver, T. Hadzic, and G. M. Whitesides, Science **284**, 948 (1999).
[5] J. Tien, T. L. Breen, and G. M. Whitesides, J. Am. Chem. Soc. **120**, 12670 (1998).
[6] A. Terfort, N. Bowden, and G. M. Whitesides, Nature (London) **386**, 162 (1997).
[7] D. H. Gracias, J. Tien, T. L. Breen, C. Hsu, and G. M. Whitesides, Science **289**, 1170 (2000).
[8] H.-J. Yeh and J. S. Smith, Proceedings of the IEEE International Workshop on Microelectromechanical Systems, Oiso, Japan, 25–29 January 1994.
[9] M. B. Cohn, K. F. Bohringer, J. M. Noworolski, A. Singh, C. G. Keller, K. Y. Goldberg, and R. T. Howe, Proc. SPIE **3513**, 2 (1998).
[10] J. J. Jacobsen, M. A. Hadley, and G. S. W. Craig, U.S. Patent No. 6,281,038 (28 August 2001).
[11] P. W. Green, R. R. A. Syms, and E. M. Yeatman, J. Microelectromech. Syst. **4**, 170 (1995).
[12] K. F. Harsh, V. M. Bright, and Y. C. Lee, Sens. Actuators A **77**, 237 (1999).
[13] D. Sohn, J. Magn. Magn. Mater. **173**, 305 (1997).
[14] M. B. Cohn, U.S. Patent No. 5,355,577 (18 October 1994).
[15] M. M. Burns, J.-M. Fournier, and J. A Golovchenko, Science **249**, 749 (1990).
[16] B. Grzybowski, H. A. Stone, and G. M. Whitesides, Nature (London) **405**, 1033 (2000).
[17] D. H. Gracias, V. Kavthekar, J. C. Love, K. E. Paul, and G. M. Whitesides, Adv. Mater. **14**, 235 (2001).